A Decomposed Co-design Strategy for Continuously Variable Transmission Design

Please check the document version of this publication:

A Decomposed Co-design Strategy for Continuously Variable Transmission Design

Chyannie A. Fahdzyana, Mauro Salazar, Theo Hofman

Abstract— This paper presents a decomposed co-design optimization framework to jointly design the geometry and the controller of a Continuously Variable Transmission (CVT), accounting for its low-level dynamics. Specifically, we first devise a model of the CVT and the feedback controller, and use it to formulate the optimal co-design problem with the goal of minimizing the transmission's mass as well as the losses that occur in the system, including the lower-level actuation. Second, we divide the resulting nonlinear multi-objective optimization problem into separate hierarchical optimization subproblems and we leverage the concept of Analytical Target Cascading (ATC) to solve the separate optimization subproblems using an interior-point optimization algorithm. Finally, we showcase our framework on a representative drive cycle. Our results demonstrate that the presented co-design method can achieve a more compact CVT design without compromising the desired ratio trajectory and reducing the overall losses by up to 14%.

I. INTRODUCTION

DEMANDS on reducing the cost of ownership of vehicles as well as their energy consumption have increased significantly over the past decade. In order to meet this design requirement, optimal vehicle design strategies have been well researched in the literature, including the development of suitable energy management control strategies [1], [2], and in combination with optimal powertrain component sizing [3].

One way to achieve an efficient vehicle energy consumption is by utilizing a Continuously Variable Transmission (CVT), which allows the primary power source to be operated at the operating points that correspond to the highest energy efficiency regions [4], [5], which then results in an improved vehicle driveline energy consumption. The general CVT shown in Fig. 1 is comprised of several subsystems, namely a variator that consists of a set of conical pulley sheaves and a belt to transmit power from the propulsion source; an actuation system, which is connected to the variator system and actuates the pulley sheaves during CVT operation; and the control subsystems, ensuring that the transmission meets the required performance. While a CVT in theory can realize an improved powertrain energy consumption, this transmission still has a significant drawback: Compared to other types of vehicle transmission, a belt-driven CVT has a relatively lower efficiency (84%), whereas a manual (MT) and automatic transmissions (AT) typically have a system efficiency of around 96% and 85%, respectively [6]. One of the main contributors of the CVT's energy consumption is the actuation system. Against this backdrop, our paper proposes an optimization framework to co-design CVTs, accounting for their actuation system.
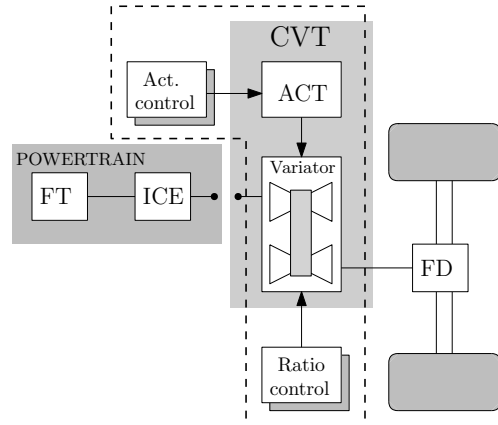
Fig. 1. Schematic diagram of the considered CVT equipped powertrain system that consists of an internal combustion engine (ICE), a fuel tank (FT), a final drive ratio (FD), as well as a CVT as the transmission system, consisting of the variator, actuation (ACT), as well as their respective controls. The system subject to co-design is denoted by the dashed black line, which includes the design of the multiple subsystems (i.e., variator and actuation) that make up the transmission.

A. Literature Review

Several integrated plant and control system design methods have been proposed in literature [7], [8]. For large-scale systems that consist of multiple components, the implementation of a simultaneous co-design method may not always be feasible due to memory limitations. A possible solution to overcome this challenge is by partitioning the problem into multiple subproblems, which is not uncommon in traditional system design. However, due to the dependency between the corresponding subsystems, solving the smaller design tasks must be properly coordinated in order to achieve the optimal design [9]. In the field of system design optimization with multiple subsystems, researchers have studied different decomposition methods for optimal system design, including Multidisciplinary Design Optimization [10], [11] and Analytical Target Cascading (ATC) [12], [13]. In particular, ATC has been shown to be an effective coordination method of decomposed optimization strategies [14], [15].

In the context of powertrain optimization, researchers have leveraged derivative-free optimization methods [16], [17], as well as convex optimization algorithms [18], [19]. Yet, these methods do not explicitly consider the design of the transmission (i.e., its physical properties and the controller). In order to improve the CVT energy efficiency and performance, several approaches have been proposed in the literature, including physically redesigning the CVT [20] and

formulating an advanced control strategy for the system [21]. However, there is no framework that can concurrently design the CVT's geometry and control, whilst accounting for its low-level actuation system, where arguably a significant part of the losses occurs.

B. Statement of Contribution

To bridge this gap, we present a decomposition-based design optimization framework for CVT systems which consists of the variator and the actuation system. In a previous study [22], a simultaneous integrated plant and control design of a CVT at the variator level has been conducted. In this work, we extend the problem formulation by including the lower level actuation system controller design. The proposed design problem is solved using a decomposed co-design approach spanning multiple subsystems (variator and actuation) based on the ATC design framework.

II. MODELING

This section elaborates the modeling and the description of the design subject. By horizontally moving the pulley sheaves on both the primary and secondary sides, the ratio of the input and output speed of a CVT is varied, which is done by the actuation system. A more detailed modeling of a CVT and its working principles can be found in [22], [23]. From now on, for the sake of simplicity, we drop the notation of time dependence whenever it is clear from the context.

Below, we focus on the description of the electro-hydraulic actuation system depicted in Fig. 2. This type of actuation system consists of two servomotor-actuated pumps, namely a shifting pump and a clamping pump. In order to horizontally move the pulley sheaves and provide the required transmission ratio during operation, the shifting pump generates a pressure p_{sh} that must match the primary clamping pressures p_{p}. Consequently, the clamping pump, which is connected to the oil reservoir, supplies a pressure p_{cl} that must match the required secondary pulley clamping pressure p_{s} to prevent the belt from slipping. Hence, in this case, the pressures generated by the pumps should be able to match the clamping pressures required at the variator level (i.e., $p_{\mathrm{p}} = p_{\mathrm{sh}}$ and $p_{\mathrm{s}} = p_{\mathrm{cl}}$, as shown in Fig. 2). This indicates the coupling between the variator and the actuation subsystems.

A. Actuation System Dynamics

The dynamics of the electro-hydraulic actuation system is expressed as

$$\dot{p}_{\mathrm{sh}} = \frac{E_{\mathrm{sh}}}{V_{\mathrm{sh}}}(V_{\mathrm{e,sh}}\omega_{\mathrm{sh}} - A_{\mathrm{p}}v_{\mathrm{p}} - Q_{\mathrm{l,sh}}) \tag{1}$$

$$\dot{p}_{\mathrm{cl}} = \frac{E_{\mathrm{cl}}}{V_{\mathrm{cl}}}(-V_{\mathrm{e,cl}}\omega_{\mathrm{cl}} - V_{\mathrm{e,sh}}\omega_{\mathrm{sh}} - A_{\mathrm{s}}v_{\mathrm{s}} - Q_{\mathrm{l,cl}}) \tag{2}$$

$$\dot{\omega}_{\mathrm{sh}} = \frac{1}{J_{\mathrm{sh}}}(T_{\mathrm{sh}} + V_{\mathrm{e,sh}}(p_{\mathrm{p}} - p_{\mathrm{s}}) - b\omega_{\mathrm{sh}} - T_{\mathrm{l,sh}}) \tag{3}$$

$$\dot{\omega}_{\mathrm{cl}} = \frac{1}{J_{\mathrm{cl}}}(T_{\mathrm{cl}} + V_{\mathrm{e,cl}}(p_{\mathrm{s}} - p_{\mathrm{atm}}) - b\omega_{\mathrm{cl}} - T_{\mathrm{l,cl}}), \tag{4}$$
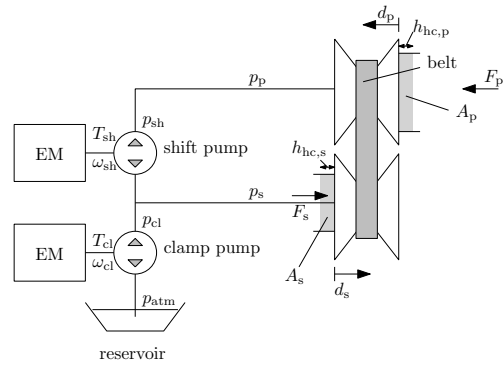

Fig. 2. Schematic diagram of an electrohydraulically actuated CVT system. It consists of a pair of servomotors (EM) that actuate the shifting and clamping pumps. The servomotors provide the torque T_{sh}, T_{cl} and rotational speed ω_{sh}, ω_{cl} necessary to prompt the pumps. The pumps supply the required pressures p_{sh} and p_{cl} that should match the required clamping pressures p_{p} and p_{s}.

where p_{sh} and p_{cl} denote the pressure generated by the shifting and clamping pumps, respectively. ω_{sh} and ω_{cl} are the shifting and clamping pump rotational speed which is supplied by the servomotors. v_{p} and v_{s} are the primary and secondary pulley displacement speed. E_i is the bulk modulus of the oil, $V_{\mathrm{e},i}$ is the pump displacement volume, J_i is the servomotor inertia, ω_i is the servomotor rotational speed, T_i is the motor torque, and b is the motor friction coefficient for $i \in \{\mathrm{sh}, \mathrm{cl}\}$. Furthermore, $Q_{\mathrm{l},i}$ and $T_{\mathrm{l},i}$ are the pump flow and torque losses which will be elaborated in the next subsection. Additionally, the effective volumes of the pulley compartments are given by

$$V_i = V_{\mathrm{o},i} + d_i A_i + C_{\mathrm{d},i} E_i, \tag{5}$$

where $V_{\mathrm{o},i}$ is the static volume of the pulley hydraulic chambers, A_i is the variator pulley surface areas, d_i is the pulley displacement, $C_{\mathrm{d},i}$ denotes the deformation capacitance of the pulley compartment and is assumed to be constant. The static volume of the hydraulic chambers is modeled as a linearly dependent function of the surface areas A_i as

$$V_{\mathrm{o},i} = A_i h_{\mathrm{hc},i}, \tag{6}$$

where $h_{\mathrm{hc},i}$ is the constant height/thickness of the hydraulic pulley chambers. As can be seen from the formulations in (1)–(4), there is also a linkage between the actuation system dynamics and the variator design (i.e., the actuation dynamics depends on the pulley surface area which is subject to design). This strengthens the motivation to perform the design of a complete system in an integrated manner where the coupling/dependency between subsystems is accounted for.

B. Actuation Losses

Here, the losses at the actuation level are those generated by the gear pumps. Such losses are due to flow and hydromechanical losses of the pumps, and are given by

$$P_{\mathrm{l,pump}} = P_{\mathrm{l,flow}} + P_{\mathrm{l,hm}}, \tag{7}$$

where the flow loss is modeled as

$$P_{\mathrm{l,flow}} = \sum_{i \in \{\mathrm{sh,cl}\}} Q_{\mathrm{l},i} \Delta p_i \, , \qquad (8)$$

whereby p_i is the pump-generated pressures, and $Q_{\mathrm{l},i}$ is the pump flow losses for $i \in \{\mathrm{sh,cl}\}$, referring to the shifting and clamping pumps, respectively. Furthermore, the hydromechanical losses are given by

$$P_{\mathrm{l,hm}} = \sum_{i \in \{\mathrm{sh,cl}\}} T_{\mathrm{l},i} \omega_{\mathrm{i}} \, , \qquad (9)$$

which depend on the pump torque losses and the rotational speed. The flow losses $Q_{\mathrm{l},i}$ (L/min or m^3/s) of the pumps are expressed as functions of the pressures, such that

$$Q_{\mathrm{l},i} = C_{\mathrm{s}} \frac{V_{\mathrm{e}} \Delta p_i}{2\pi \mu_{\mathrm{f}}} + C_{\mathrm{p}} p_{\mathrm{in},i} \, , \qquad (10)$$

where V_{e} is the pump displacement volume (m^3/rad), μ_{f} is the fluid viscosity constant. The corresponding pump pressure difference Δp_i is expressed as

$$\Delta p_i = \begin{cases} p_{\mathrm{p}} - p_{\mathrm{s}} & \text{for } i = \mathrm{sh} \\ p_{\mathrm{s}} - p_{\mathrm{atm}} & \text{for } i = \mathrm{cl} \, . \end{cases} \qquad (11)$$

Additionally, the input pressures corresponding to the pumps are given by

$$p_{\mathrm{in},i} = \begin{cases} \min\{p_{\mathrm{p}}, p_{\mathrm{s}}\} & \text{for } i = \mathrm{sh} \\ \min\{p_{\mathrm{s}}, p_{\mathrm{atm}}\} & \text{for } i = \mathrm{cl} \, . \end{cases} \qquad (12)$$

Furthermore, the torque losses $T_{\mathrm{l},i}$ that contribute to the hydromechanical losses are expressed as a function of the pressures as well as the servomotor rotational speed, such that

$$T_{\mathrm{l},i} = C_{\mathrm{f}} \frac{V_{\mathrm{e},i} \Delta p_i}{2\pi \mu_{\mathrm{f}}} + C_{\mathrm{d}} \mu_{\mathrm{f}} V_{\mathrm{e},i} \omega_i^2 + C_{\mathrm{in}} V_{\mathrm{e},i} p_{\mathrm{in}} \, , \qquad (13)$$

where the coefficients C_{s}, C_{p}, C_{f}, C_{d}, and C_{in} are fitted parameters obtained from measurement.

III. METHODOLOGY

We present a decomposed co-design strategy for CVT variator and actuation system design based on an ATC framework. We divide the integrated system design problem into two separate hierarchical optimization subproblems. A more detailed formulation of a general ATC framework can be found in [12].

A. CVT Co-design Objective

The objective of the CVT co-design problem is to minimize the transmission mass as well as the losses that occur in the system (i.e., the leakage and the actuation system losses). The plant design parameters are the variator parameters $\mathbf{x}_{\mathrm{P}} = [\beta, R_1, R_2]$, and the control design parameters $\mathbf{x}_{\mathrm{C}}$ include the variator controller gains K_{p} and K_{i}, as well as the optimized servomotor torques T_{sh} and T_{cl}, such that $\mathbf{x}_{\mathrm{C}} = [K_{\mathrm{p}}, K_{\mathrm{i}}, T_{\mathrm{sh}}, T_{\mathrm{cl}}]$. More details on the derivation of the corresponding models of the variator design problem are

discussed in [22]. In this work, the complete CVT system design problem is stated as

$$\min_{\mathbf{x}_{\mathrm{P}}, \mathbf{x}_{\mathrm{C}}} w_{\mathrm{P}} M_v(\mathbf{x}_{\mathrm{P}}) + \int_0^{t_{\mathrm{f}}} w_{\mathrm{C1}} P_{\mathrm{l}}(\mathbf{x}_{\mathrm{P}}, \mathbf{x}_{\mathrm{C}}) + w_{\mathrm{C2}} P_{\mathrm{l,pump}}(\mathbf{x}_{\mathrm{P}}, \mathbf{x}_{\mathrm{C}}) \, \mathrm{d}t \qquad (14a)$$

subject to:

$$\beta \in [\underline{\beta}, \overline{\beta}], R_1 \in [\underline{R}_1, \overline{R}_1], R_2 \in [\underline{R}_2, \overline{R}_2], \qquad (14b)$$

$$\dot{r}_{\mathrm{g}}(t) = 2\omega_{\mathrm{p}}(t) \Delta \frac{1 + \cos^2(\beta)}{\sin(2\beta)} c(r_{\mathrm{g}}(t)) u(t), \qquad (14c)$$

$$P_{\mathrm{l,var}}(t) = C_{\mathrm{l,p}} p_{\mathrm{p}}^2(t) + C_{\mathrm{l,s}} p_{\mathrm{s}}^2(t), \qquad (14d)$$

$$p_{\mathrm{p}}(t) = \frac{F_{\mathrm{p}}(t) - F_{\mathrm{cf,p}}(t)}{A_{\mathrm{p}}}, \qquad (14e)$$

$$p_{\mathrm{s}}(t) = \frac{F_{\mathrm{s}}(t) - F_{\mathrm{cf,s}}(t) - F_{\mathrm{spr}}(t)}{A_{\mathrm{s}}} \qquad (14f)$$

$$F_{\mathrm{spr}} = F_{\mathrm{spr,o}} + k_{\mathrm{spr}}(\overline{d}_{\mathrm{s}} - d_{\mathrm{s}}) \qquad (14g)$$

$$A_{\mathrm{p}} = \pi(r_{\mathrm{po,p}}^2 - r_{\mathrm{pi,p}}^2), A_{\mathrm{s}} = \pi(r_{\mathrm{po,s}}^2 - r_{\mathrm{pi,s}}^2), \qquad (14h)$$

$$F_{\mathrm{cf,p}}(t) = \frac{\pi}{4} \rho_{\mathrm{o}} (r_{\mathrm{po,p}}^4 - r_{\mathrm{in,p}}^4) \omega_{\mathrm{p}}^2(t), \qquad (14i)$$

$$F_{\mathrm{cf,s}}(t) = \frac{\pi}{4} \rho_{\mathrm{o}} (r_{\mathrm{po,s}}^4 - r_{\mathrm{in,s}}^4) \omega_{\mathrm{s}}^2(t), \qquad (14j)$$

$$F_{\mathrm{s}}(t) = \frac{\cos(\beta) (|T_{\mathrm{P}}(t)| + S_{\mathrm{f}} T_{\mathrm{max}})}{2\,\overline{\mu}_{\mathrm{cvt}} R_{\mathrm{p}}}(t), \qquad (14k)$$

$$F_{\mathrm{p}}(t) = \exp \left[u(t) + \ln \left(\left. \frac{F_{\mathrm{p}}}{F_{\mathrm{s}}}(t) \right|_{\mathrm{ss}} \right) \right] F_{\mathrm{s}}(t), \qquad (14l)$$

$$u(t) = \frac{u_{\mathrm{n}}(t)}{2\,\omega_{\mathrm{p}}(t) \Delta \frac{1 + \cos^2(\beta)}{\sin(2\beta)} c(r_{\mathrm{g}}(t))} \qquad (14m)$$

$$u_{\mathrm{n}}(t) = -K_{\mathrm{p}} e(t) - K_{\mathrm{i}} \int_0^t e(\tau) \, \mathrm{d}\tau, \qquad (14n)$$

$$e(t) = r_{\mathrm{g}}(t) - r_{\mathrm{g,r}}(t), \qquad (14o)$$

$$P_{\mathrm{l,pump}} = \sum_{i \in \{\mathrm{sh,cl}\}} Q_{\mathrm{l},i} \Delta p_i + \sum_{i \in \{\mathrm{sh,cl}\}} T_{\mathrm{l},i} \omega_i, \qquad (14p)$$

$$\dot{p}_{\mathrm{sh}} = \frac{E_{\mathrm{sh}}}{V_{\mathrm{sh}}} (V_{\mathrm{e,sh}} \omega_{\mathrm{sh}} - A_{\mathrm{p}} v_{\mathrm{p}} - Q_{\mathrm{l,sh}}) \qquad (14q)$$

$$\dot{p}_{\mathrm{cl}} = \frac{E_{\mathrm{cl}}}{V_{\mathrm{cl}}} (-V_{\mathrm{e,cl}} \omega_{\mathrm{cl}} - V_{\mathrm{e,sh}} \omega_{\mathrm{sh}} - A_{\mathrm{s}} v_{\mathrm{s}} - Q_{\mathrm{l,cl}}) \qquad (14r)$$

$$\dot{\omega}_{\mathrm{sh}} = \frac{1}{J_{\mathrm{sh}}} (T_{\mathrm{sh}} + V_{\mathrm{e,sh}}(p_{\mathrm{p}} - p_{\mathrm{s}}) - b\omega_{\mathrm{sh}} - T_{\mathrm{l,sh}}) \qquad (14s)$$

$$\dot{\omega}_{\mathrm{cl}} = \frac{1}{J_{\mathrm{cl}}} (T_{\mathrm{cl}} + V_{\mathrm{e,cl}}(p_{\mathrm{s}} - p_{\mathrm{atm}}) - b\omega_{\mathrm{cl}} - T_{\mathrm{l,cl}}), \qquad (14t)$$

where the actuation losses $P_{\mathrm{l,pump}}$ are described in (7)–(13).

B. Formulation of the Decomposed Co-design Approach

We divide the combined CVT integrated design problem into two separate hierarchical optimization subproblems. The upper stage subproblem is related to solving the design problem at the variator level, that is determining the required clamping pressures during CVT operation, while simultaneously minimizing the discrepancy between the target and response variables. The lower stage optimization subproblem finds the optimal servomotor torques needed to operate the shifting and clamping pumps at the actuation level, while also minimizing the losses that occur as well as the disparity between the shared variables of the subproblems.

The shared or linking variables are those that appear in the constraints or objective functions of the decomposed subproblems. In this work, the linking variables $\mathbf{z}$ between the subproblems are the primary and secondary clamping

$$\min_{\mathbf{x}_P, \mathbf{x}_{C1}} w_P \, M_v(\mathbf{x}_P) + \int_0^{t_f}(w_{C1}P_{l,var}(\mathbf{x}_P, \mathbf{x}_{C1}) + w_1(p_{sh}^L - p_p)^2 + w_2(p_{cl}^L - p_s)^2$$
$$+ w_3(r_g^L - r_g)^2)dt + w_4(\beta^L - \beta)^2 + w_5(R_1^L - R_1)^2 + w_6(R_2^L - R_2)^2,$$
$$\text{s.t. } (14b)\text{-}(14o)$$

p_p^U, p_s^U, r_g^U
β^U, R_1^U, R_2^U

$p_{sh}^L, p_{cl}^L, r_g^L$
β^L, R_1^L, R_2^L

$$\min_{\mathbf{x}_{C2}} \int_0^{t_f}(w_{C2}P_{l,pump}(\mathbf{x}_P, \mathbf{x}_{C2}) + w_1(p_p^U - p_{sh})^2 + w_2(p_s^U - p_{cl})^2$$
$$+ w_3(r_g^U - r_g)^2)dt + w_4(\beta^U - \beta)^2 + w_5(R_1^U - R_1)^2 + w_6(R_2^U - R_2)^2,$$
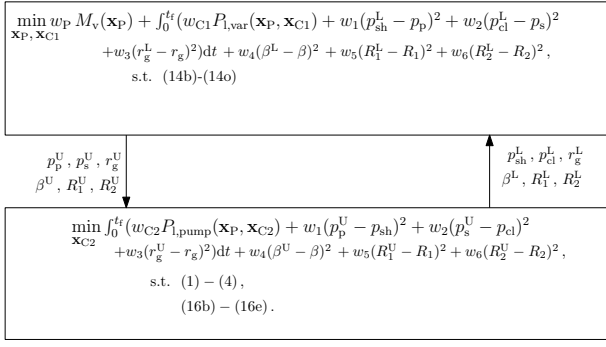$$\text{s.t. } (1) - (4),$$
$$(16b) - (16e).$$

Fig. 3. The ATC-based decomposed co-design problem presented in this paper. The higher level subproblem minimizes the variator mass and leakage losses, as well as the discrepancy between the shared variables. The results of this optimization subproblem is passed down to the lower level subproblem, which minimizes the actuation system losses as well as the discrepancy between the shared variables.

pressures p_p and p_s, shifting and clamping pressures p_{sh} and p_{cl}, the CVT ratio trajectory r_g, as well as the CVT geometrical parameters β, R_1, and R_2. The proposed decomposed optimization scheme is shown in Fig. 3.

1) Upper level optimization subproblem: Mathematically, the upper level optimization problem in discrete time is stated as follows:

$$\min_{\mathbf{x}_P, \mathbf{x}_{C1}} w_P \, M_v(\mathbf{x}_P) + \int_0^{t_f}(w_{C1}P_{l,var}(\mathbf{x}_P, \mathbf{x}_{C1}) + w_1(p_{sh}^L - p_p)^2$$
$$+ w_2(p_{cl}^L - p_s)^2 + w_3(r_g^L - r_g)^2)dt + w_4(\beta^L - \beta)^2$$
$$+ w_5(R_1^L - R_1)^2 + w_6(R_2^L - R_2)^2,$$
(15a)

subject to (14b)–(14t). $\mathbf{x}_P$ represents the variator plant design parameters $\mathbf{x}_P = [\beta, R_1, R_2]$, $\mathbf{x}_{C1}$ is the set of control design parameters of the upper level subproblem defined as $\mathbf{x}_{C1} = [K_p, K_i]$. In addition to the original variator level optimization problem, the upper level also minimizes the discrepancy between the shared variables of the two subproblems $\mathbf{z} = [p_p, p_s, p_{sh}, p_{cl}, r_g, \beta, R_1, R_2]$. The parameters indicated by superscript L are generated by the lower level subproblem, and are treated as constants in this optimization subproblem.

2) Lower level optimization subproblem: At the lower level, the optimization problem consists of minimizing the actuation system losses with respect to the control design parameters at the lower level (i.e., $\mathbf{x}_{C2} = [T_{sh}, T_{cl}]$), as well as the difference between the shared variables. The optimization problem formulation is given by

$$\min_{\mathbf{x}_{C2}} \int_0^{t_f}(w_{C2}P_{l,pump}(\mathbf{x}_P, \mathbf{x}_{C2}) + w_1(p_p^U - p_{sh})^2 + w_2(p_s^U - p_{cl})^2$$
$$+ w_3(r_g^U - r_g)^2)dt + w_4(\beta^U - \beta)^2 + w_5(R_1^U - R_1)^2$$
$$+ w_6(R_2^U - R_2)^2,$$
(16a)

subject to the dynamics of the actuation system expressed in (1)–(4), as well as the constraints on the state and input

variables of the actuation system dynamics:

$$\underline{\omega}_{sh} \le \omega_{sh}(t) \le \overline{\omega}_{sh}, \qquad \forall t \in [0, t_f], \tag{16b}$$
$$\underline{\omega}_{cl} \le \omega_{cl}(t) \le \overline{\omega}_{cl}, \qquad \forall t \in [0, t_f], \tag{16c}$$
$$\underline{T}_{sh} \le T_{sh}(t) \le \overline{T}_{sh}, \qquad \forall t \in [0, t_f], \tag{16d}$$
$$\underline{T}_{cl} \le T_{cl}(t) \le \overline{T}_{cl}, \qquad \forall t \in [0, t_f]. \tag{16e}$$

The decomposed co-design optimization framework is performed in an iterative manner. First, we start by initializing the values of the target shared variables $\mathbf{z}^U = [p_p^U, p_s^U, p_{sh}^U, p_{cl}^U, r_g^U, \beta^U, R_1^U, R_2^U]$ and solve the lower level subproblem utilizing these initial values. Then, using the optimized values of $\mathbf{z}^L$ returned by the lower level, we solve the upper level optimization problem. This completes one iteration. The iterative process is repeated until the termination criterion is reached, that is when the discrepancies between the shared variables are within a desired tolerable value, given by

$$\frac{1}{t_f} \int_0^{t_f} \left(\left(\frac{p_p^U - p_{sh}^L}{p_p^U} \right)^2 + \left(\frac{p_s^U - p_{cl}^L}{p_s^U} \right)^2 + \left(\frac{r_g^U - r_g^L}{r_g^U} \right)^2 \right) dt$$
$$+ \left(\frac{\beta^U - \beta^L}{\beta^U} \right)^2 + \left(\frac{R_1^U - R_1^L}{R_1^U} \right)^2 + \left(\frac{R_2^U - R_2^L}{R_2^U} \right)^2 \le \epsilon$$
(17)

where ϵ is the user-defined maximum tolerance of the discrepancies between the target and response variables. Small value of ϵ enforces the shared variables of the top and bottom level to not deviate from each other, ultimately yielding trustworthy results.

IV. RESULTS

This section discusses the results stemming from the proposed co-design approach. We discretize the subsystems' dynamics with the Euler Forward method. The decomposed optimization subproblems are parsed with CasADi [24] and solved using the IPOPT solver [25] provided by the OPTI toolbox for the Python interface.

We observed that the optimization problem present in this paper is of a nonlinear nature, hence different initial values can influence the obtained optimization results. The selection of the error tolerance can also affect the performance of the optimization framework. The tighter the tolerance, the more iterations it takes for the decomposed optimization to converge. Selecting the tolerance value ϵ depends on the design problem and should be done carefully, as too large a value may result in premature convergence, whilst using an ϵ that is too small may cause convergence issues. Moreover, it was found that the total computation time of the proposed optimal design framework depends on the number of iterations that the subproblems take to converge, and ultimately relies on the initial values supplied at the start of the algorithm, the complexity and the scale of the design problem, as well as the coupling strength between the subproblems.

The optimized design results presented in this section are obtained over a selected dynamic cycle, namely, the New European Drive Cycle (NEDC). In this study, we consider an
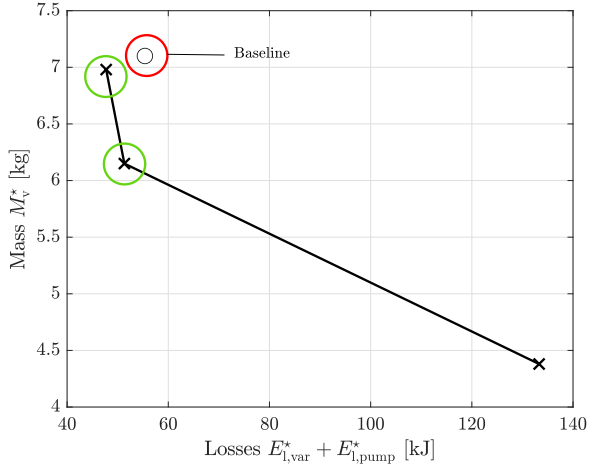
Fig. 4. Pareto front of the proposed design optimization problem and baseline solution.
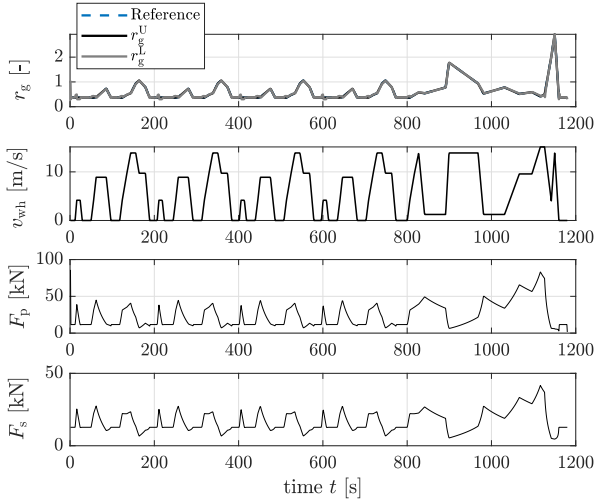

Fig. 5. Plot of the resulting performance of the optimized CVT design over the NEDC.
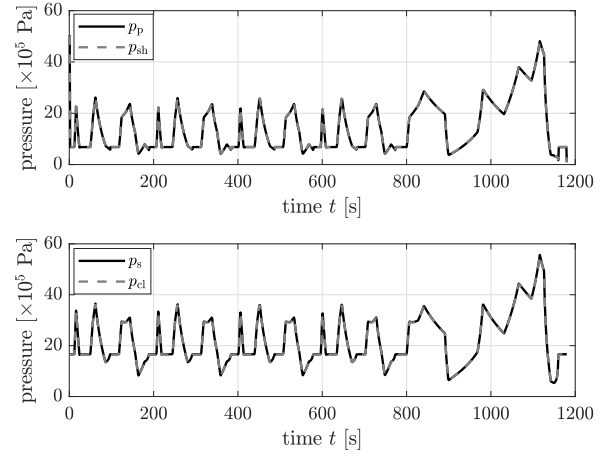

Fig. 6. Target and response pressure variables of the decomposed optimization problem.

TABLE I

Optimization results utilizing the proposed decomposition framework

Description	Parameters	Baseline	Decomposed	Decomposed	Decomposed	Unit
Opt. weight	w_P	-	1e6	1e-5	1e6	kg^{-1}
Opt. weight	w_C	-	1e-5	1e5	1e-4	J^{-1}
Opt. weight	w_C2	-	0.01	10	1e-4	J^{-1}
Opt. weight	w_1	-	1e-3	1e-3	1e-5	10^{-5}s^{-1}Pa^{-2}
Opt. weight	w_2	-	1e-3	1e-3	1e-5	10^{-5}s^{-1}Pa^{-2}
Opt. weight	w_3	-	100	500	100	s^{-1}
Opt. weight	w_4	-	1e6	1e6	1e6	deg^{-2}
Opt. weight	w_5	-	1e6	1e6	1e6	mm^{-2}
Opt. weight	w_6	-	1e6	1e6	1e6	mm^{-2}
Variator mass	$M_\mathrm{v}^\star$	7.1	6.15	6.98	4.38	kg
Wedge angle	$\beta^\star$	11	7	9.32	7	deg
Shaft radius	$R_1^\star$	23.5	27	27	21.3	mm
Pulley radius	$R_2^\star$	85.5	88	88.5	72.87	mm
Proportional gain	$K_\mathrm{P}^\star$	3.62	0.078	5	4.99	$\cdot 10^2$
Integral gain	$K_\mathrm{i}^\star$	4.99	0.06	5	4.99	$\cdot 10^2$
Pump losses	$E_{\mathrm{l,pump}}^\star$	33	29	28.36	54.7	kJ
Var. leakage losses	$E_{\mathrm{l,var}}^\star$	22.37	22.2	19.36	78.55	kJ
Total losses	$E_\mathrm{l}^\star$	55.38	51.32	47.72	133.3	kJ
Simulation time	T_sim	-	367.7	205.7	152.3	s

internal combustion engine vehicle. Thereby, we generate a reference CVT ratio trajectory $r_\mathrm{g,ref}(t)$ operating the engine at the Optimal Operation Line (OOL), i.e.,

$$r_\mathrm{g,ref}(t) = \frac{\omega_\mathrm{wh}(t)}{\omega_\mathrm{e}^\star(t) \cdot r_\mathrm{fd}}, \qquad (18)$$

whereby $\omega_\mathrm{wh}(t)$ is the required wheel rotational speed that is determined by the drive cycle, r_fd is the final drive ratio, which is chosen as a constant, and $\omega_\mathrm{e}^\star(t)$ is the optimal engine speed yielding the minimum fuel consumption. Here, we depict the results obtained for $w_\mathrm{P} = 1e-5$, $w_\mathrm{C1} = 1e5$, $w_\mathrm{C2} = 10$, and $\mathbf{w} = [w_1, w_2, ..., w_6] = [1e-3, 1e-3, 500, 1e6, 1e6, 1e6]$ in Fig. 5 to Fig. 7. The results of the proposed design framework for different values of weighting parameters are summarized in Table I. Additionally, the results are compared to a baseline design of a commercial CVT available for passenger cars.

Fig. 4 depicts the Pareto front stemming from the proposed optimization problem for various optimization weights. When more emphasis is placed on minimizing the losses, the transmission mass gets larger, and vice versa, indicating a trade-off between the plant and control objectives. Crucially, our framework can significantly outperform the baseline solution with regard to both the losses and the mass (cf. the solution marked in green in Fig. 4): The realized CVT designs are 13% and 2% lighter in terms of variator mass, whilst resulting in 7% and 14% reductions in losses, respectively.

We can discern from Fig. 5 that the optimized CVT design is capable of accurately realizing the desired ratio trajectory yielding minimum energy consumption. Furthermore, it is also visible that the shared variables between the decomposed optimization subproblems converge to the same values, as shown in Fig. 6. In fact, the proposed decomposed optimization framework takes 3 iteration steps before converging, as depicted in Fig. 7.

V. Conclusions

In this paper, we have presented the results of a decomposed co-design approach for a Continuously Variable Transmission (CVT), whereby we optimized its geometry
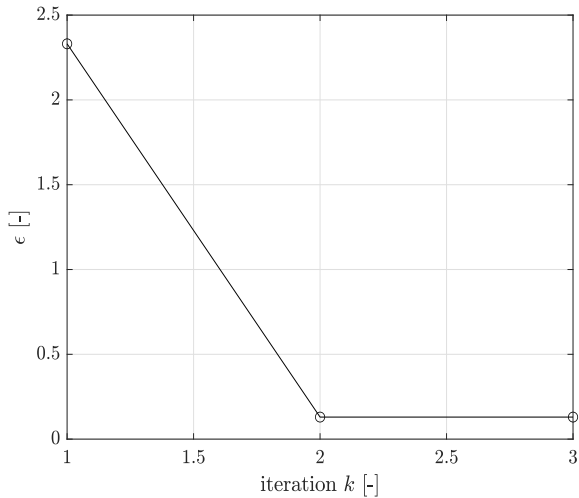
Fig. 7. Discrepancy between the target and response variables of the decomposed optimization problem.

and actuation system jointly with its feedback controller. We demonstrated that our proposed approach is capable of solving the multi-level CVT co-design problem consisting of variator and actuation system. Specifically, the co-design approach presented in this work leveraged Analytical Target Cascading (ATC) to dissect the optimal CVT variator and actuation system co-design problem into two separate sub-problems by exploiting the hierarchy present in the system. All in all, our framework enabled us to show that, with respect to a baseline, it is possible to achieve a more compact and efficient design, reducing losses by up to 14%.

In the future, we are interested in comparing the results of the proposed design framework with that of traditional system design, namely sequential methods and/or iterative strategies. Furthermore, possible extensions of this research line could incorporate the design optimization of a complete vehicle powertrain system, finding the optimal sizing of the components and the energy management, and designing the optimal CVT (the physical parameters and the corresponding controllers over the multiple subsystems) suitable for the vehicle under consideration.

VI. Acknowledgement

References

[1] T. Hofman, M. Steinbuch, R. Van Druten, and A. Serrarens, "Rule-based energy management strategies for hybrid vehicles," *International Journal of Electric and Hybrid Vehicles*, vol. 1, no. 1, pp. 71–94, 2007.

[2] N. Robuschi, M. Salazar, P. Duhr, F. Braghin, and C. H. Onder, "Minimum-fuel engine on/off control for the energy management of hybrid electric vehicles via iterative linear programming," in *Symposium on Advances in Automotive Control*, 2019.

[3] L. Wang, E. Collins, and H. Li, "Optimal design and real-time control for energy management in electric vehicles," *IEEE Transactions on Vehicular Technology*, vol. 60, no. 4, pp. 1419 – 1429, 2011.

[4] T. Hofman and M. Salazar, "Transmission ratio design for electric vehicles via analytical modeling and optimization," in *IEEE Vehicle Power and Propulsion Conference*, 2020, in press.

[5] O. Borsboom, C. A. Fahdzyana, M. Salazar, and T. Hofman, "Time-optimal control strategies for electric race cars for different transmission technologies," in *IEEE Vehicle Power and Propulsion Conference*, 2020, in press.

[6] M. A. Kluger and D. M. Long, "An overview of current automatic, manual and continuously variable transmission efficiencies and their projected future improvements," in *SAE World Congress*, 1999.

[7] H. Fathy, "Combined plant and control optimization: Theory, strategies and applications," Ph.D. dissertation, Univ. of Michigan, 2003.

[8] J. Allison, "Optimal partitioning and coordination decisions in decomposition-based design optimization," Ph.D. dissertation, Univ. of Michigan, 2008.

[9] J. Reyer, "Combined embodiment design and control optimization: Effects of cross-disciplinary coupling," Ph.D. dissertation, Univ. of Michigan, 2000.

[10] P. W. Jansen, R. E. Perez, and J. Martins, "Aerostructural optimization of nonplanar lifting surfaces," *AIAA Journal of Aircraft*, vol. 47, no. 5, pp. 1490–1503, 2010.

[11] S. Ning and I. Kroo, "Multidisciplinary considerations in the design of wings and wing tip devices," *AIAA Journal of Aircraft*, vol. 47, no. 2, pp. 534–543, 2010.

[12] Y. Kim, H, D. G. Rideout, P. Y. Papalambros, and J. Stein, "Analytical target cascading in automotive vehicle design," *ASME Journal of Mechanical Design*, vol. 125, no. 3, pp. 481–489, 2003.

[13] M. Behtash and M. J. Alexander-Ramos, "A decomposition-based optimization algorithm for combined plant and control design of inter-connected dynamic systems," *ASME Journal of Mechanical Design*, vol. 142, no. 6, p. 061703, 2020.

[14] S. Tosserams, L. F. P. Etman, P. Y. Papalambros, and J. E. Rooda, "An augmented lagrangian relaxation for analytical target cascading using the alternating direction method of multipliers," *Structural and Multidisciplinary Optimization*, vol. 31, pp. 176–189, 2006.

[15] J. T. Allison, K. M., M. R. Zawislak, and P. Y. Papalambros, "On the use of analytical target cascading and collaborative optimization for complex system design," in *World Congress of Structural and Multidisciplinary Optimization*, 2005.

[16] S. Ebbesen, P. Elbert, and L. Guzzella, "Engine downsizing and electric hybridization under consideration of cost and drivability," *Oil & Gas Science and Technology–IFP Energies Nouvelles*, vol. 68, no. 1, pp. 109–116, 2013.

[17] F. J. R. Verbruggen, E. Silvas, and T. Hofman, "Electric powertrain topology analysis and design for heavy-duty trucks," *Energies*, vol. 13, no. 10, 2020.

[18] N. Murgovski, L. Johannesson, X. Hu, B. Egardt, and J. Sjoberg, "Convex relaxations in the optimal control of electrified vehicles," in *American Control Conference*, 2015.

[19] F. J. R. Verbruggen, M. Salazar, M. Pavone, and T. Hofman, "Joint design and control of electric vehicle propulsion systems," in *European Control Conference*, 2020.

[20] T. W. G. L. Klaassen, "The empact cvt: dynamics and control of an electromechanically actuated cvt," Ph.D. dissertation, Eindhoven University of Technology, 2007.

[21] B. Bonsen, "Efficiency optimization of the push-belt cvt by variator slip control," Ph.D. dissertation, Eindhoven University of Technology, 2006.

[22] C. Fahdzyana, M. Salazar, and T. Hofman, "Integrated plant and control design of a continuously variable transmission," submitted to IEEE Transactions on Vehicular Technology.

[23] C. Fahdzyana, S. van Raemdonck, and T. Hofman, "Joined plant and control design for continuous variable transmission systems," in *American Control Conference*, 2020.

[24] J. A. E. Andersson, J. Gillis, G. Horn, J. B. Rawlings, and M. Diehl, "Casadi – a software framework for nonlinear optimization and optimal control," *Mathematical Programming Computation*, vol. 11, no. 1, pp. 1–36, 2019.

[25] A. Wächter and L. Biegler, "On the implementation of a primal-dual interior point filter line search algorithm for large-scale nonlinear programming," *Mathematical Programming*, vol. 106, no. 1, pp. 25–57, 2006.